80-10-244
高エネ研図書室

Ref.TH.2918-CERN

THE 2γ REACTION $e^+e^- \to e^+e^-\pi^+\pi^-$ IN THE RESONANCE REGION

H. Krasemann and J.A.M. Vermaseren
CERN - Geneva

A B S T R A C T

In the framework of the non-relativistic quark model we calculate rates and various distributions for the reactions $e^+e^- \to e^+e^-f \to e^+e^-\pi^+\pi^-$ and $e^+e^- \to e^+e^-\varepsilon \to e^+e^-\pi^+\pi^-$, assuming that an $\varepsilon(1300)$ meson exists. The effect of the experimental acceptance is also investigated.

Ref.TH.2918-CERN
11 August 1980

1. INTRODUCTION

With e^+e^- colliders reaching a CM energy of 10 GeV or more, 2γ physics has become a readily observable and interesting field. At high invariant mass in the 2γ system, one can separate the QED background easily from the hadronic signals. The importance of these hadronic events in studying QCD was first emphasized by Brodsky et al.[1]. In the very low 2γ mass region, however, the hadronic channel is not dominated by the process $\gamma\gamma \to q\bar{q}$ but by resonance production and a $\pi\pi$ continuum. An added complication in the understanding of hadronic physics at low 2γ mass is the experimental problem of identifying which events are electromagnetic in nature and which are hadronic, as slow muons, pions and electrons cannot always be distinguished. Compared to the $\pi\pi$ continuum the QED background is more than an order of magnitude larger[2]. Nevertheless with sufficient statistics, resonances can still be observed as reported recently by PLUTO[3] and TASSO[4]. The quality of the data is expected to become much better, especially when particle identification is improved.

In this paper we will discuss possible resonance formation in the $e^+e^- \to \to e^+e^- \pi^+\pi^-$ final state. Earlier works[5] already exist on this topic but we aim to make improvements in two directions. First, we do not make any approximations in the QED part of the reaction, keeping photon polarizations and virtual masses. Secondly, instead of relating the two-photon resonance production amplitude to other processes, which introduces many ambiguities, we use the non-relativistic quark model (NRQM) to describe the formation of $q\bar{q}$ resonances by two photons. At this point we may remind the reader not only of the successes of the NRQM in describing meson-photon couplings but especially of an earlier successful application of the NRQM $f\gamma\gamma$ (or fgg) coupling in $J/\psi \to \gamma gg \to \gamma f \to \gamma\pi^+\pi^-$ decays[6]. The two photon annihilations should be a very clean process for looking for $C = +$ quark model resonances. The states expected to be produced by two photons and to decay into two pions below 2 GeV/c^2 invariant mass are the $f(1270)$ and possibly a $S^*(980)$ or $\varepsilon(1300)$. We will discuss the couplings of these states to two photons in Section 2. We rederive the spin structure of the $\gamma\gamma f$ coupling in Section 3 in terms of the non-relativistic quark model (NRQM) and compare the result to earlier work. Although for reasons of simplicity we describe the $q\bar{q}$ bound state in the zero binding limit, we take the finite width of the f (and possible ε) meson into account. It is straightforward to apply the $\gamma\gamma f$ matrix element to virtual photons, and it can be shown that within the NRQM no additional form factors enter. Section 4 tries to illuminate the helicity structure of the $f\gamma\gamma$ vertex thus obtained for timelike photons. In Section 5 we discuss some of the details of calculating the full matrix element for $e^+e^- \to e^+e^- \pi^+\pi^-$ via an

f (or ε) resonance. The kinematics and Monte Carlo integration use standard procedures[7]. Results of this integration in the form of various distributions are discussed in Section 6. The conclusions follow in the seventh and final section.

2. QUARK MODEL RESONANCES IN $\gamma\gamma \to \pi^+\pi^-$

The Feynman diagram for the process in question is displayed in Fig. 1. The two pion system is in a $C = +$ state, thus requiring even total angular momentum. It therefore also has even parity: $J^{PC} = 0^{++}, 2^{++}, \ldots$ and the G parity requires isospin $I = 0$. There are only four quark model resonances (assuming arbitrary mixing for the moment), which can contribute below 2 GeV invariant 2π mass, namely the $I = 0$ members of the $J^P = 0^+$ and 2^+ quark model nonets. These states have in common that quark spins are aligned (triplet) and that the orbital angular momentum is one, combining to a total spin $j = 0$ or 2. In the SU(3) limit the non-relativistic wave functions are therefore identical. The coupling to two photons has the well-known dependence on the expectation value of the (charge)^2 operator which reads (colour included)

$$\langle Q^2 \rangle^2_{q\bar{q}} = \frac{1}{81} \left(6 \cos\theta + \frac{3}{\sqrt{2}} \sin\theta\right)^2 \qquad (2.1)$$

when the meson quark content is (in the $(u,d,s) \times \begin{pmatrix} u \\ d \\ s \end{pmatrix}$ basis)

$$\frac{1}{\sqrt{3}} \begin{pmatrix} \cos\theta + \frac{1}{\sqrt{2}} \sin\theta & & \\ & \cos\theta + \frac{1}{\sqrt{2}} \sin\theta & \\ & & \cos\theta - \sqrt{2} \sin\theta \end{pmatrix},$$

e.g. $\theta(f) \simeq 35^\circ$ and $\theta(f') \simeq 35^\circ + 90^\circ$. Equation (2.1) is bound between 0 and 0.5 (for the f it is 0.46). Apart from the fact that the $s\bar{s}$ component of a meson cannot couple to $\pi^+\pi^-$ (this excludes the f' from contributing to the process under study), the $\langle Q^2 \rangle^2$ of two isospin zero mesons of a given nonet lie 90° apart in Eq. (2.1), which allows us to give a lower limit on the $\langle Q^2 \rangle^2_{I=0}$ of at least one of the two states of

$$\langle Q^2 \rangle^2_{I=0} \geq 0.23 \quad . \qquad (2.2)$$

By ε we will denote the $j^{PC} = 0^{++}$ meson with the same quark content as the f meson. ε' then denotes the state corresponding to the f'. Any physical 0^{++} resonance may be a mixture of ε and ε'; two candidates for these are the $S^*(980)$ and the $\varepsilon(1300)$ [8]. For the quark model ε it is well known that $\Gamma_{\varepsilon\gamma\gamma} = (15/4)\,\Gamma_{f\gamma\gamma}$. If $S^*(980)$ and $\varepsilon(1300)$ are indeed the two physical $I = 0$ $j^{PC} = 0^{++}$ mesons, then it is clear from (2.2) that either $\Gamma_{S^*(980)\gamma\gamma}$ or $\Gamma_{\varepsilon(1300)\gamma\gamma}$ must be $> (15/4) \cdot (0.23/0.46)\,\Gamma_{f\gamma\gamma}$, and is therefore likely to be seen in two-photon production (compare ch. 6). Our discussion so far has completely neglected the possibility that there might be glueball states (bound gluons) with $j^{PC} = 0^{++}$ or 2^{++}. We will not go into details here, but only remark that the glue component of a 0^{++} or 2^{++} meson is unlikely to be produced by two photons since the gluons are neutral. Together with other experiments where glueball states are likely to be seen, like $J/\psi \to \gamma X$, this argument can be turned around to determine the glue content or $q\bar{q}$ content respectively of a given resonance. The fact that a resonance does not show up in two-photon production may then indicate that this resonance is a glueball state.

3. THE AMPLITUDE FOR $\gamma\gamma \to f \to \pi\pi$ and $\gamma\gamma \to \varepsilon \to \pi\pi$

We begin with $\gamma\gamma \to f$. In principle there are five independent helicity amplitudes (the indices denote photon helicities): $A_{+-} = A_{-+}$, $A_{+0} = A_{-0}$, $A_{0+} = A_{0-}$, $A_{++} = A_{--}$, A_{00}. Since we will only discuss the process with at most one photon off mass shell, it suffices to consider A_{+-}, A_{+0}, A_{++}. For both photons on mass-shell, Yang's theorem [9] gives $A_{+0} = 0$. Finite energy sum rules (which lead to $\Gamma(f \to \gamma\gamma) \approx 3$ kev) [10] show that

$$A_{+-} \gg A_{++} \quad . \tag{3.1}$$

Describing the f meson as a non-relativistic bound state of (relatively heavy, $m_q \approx M_f/2$) quarks one has [11]

$$A_{++} = 0 \tag{3.2}$$

which agrees with Eq. (3.1).

We will describe the $\gamma\gamma \to f$ coupling in terms of a non-relativistic bound state model, i.e., we will calculate the imaginary part of the diagrams in Fig. 2, using only the large components of the f meson spin wave function and the spatial wave function in a non-relativistic approximation. The spatial part of the loop is essentially an integral over the non-relativistic wave function and results

in just one number: $R'(0)$, the derivative of the Schrödinger wave function at zero separation. The similarity of Eqs (3.1) and (3.2) encourages us to trust the analytic structure of the lowest order calculation, but mainly because of the relativistic corrections to the Schrödinger wave function, we cannot trust the $\Gamma(f \to \gamma\gamma) = 1$ keV, calculated with Eq. (3.9) . Rather we will parametrize the production of f's in two gamma collisions with $\Gamma_{f\gamma\gamma}$. Since we do trust the analytic structure of the coupling, however, we can extend the calculation to virtual (space- or timelike) photons. An idea of how much the parameter $\Gamma_{f\gamma\gamma}$ will change for off-shell photons (or: how much of an f meson form factor should be included additionally) is given by a little numerical exercise: assuming that the quarks in the f are on-shell gives $(k_1 - P/2)^2 \approx -m_q^2$ for the (virtual mass)^2 of the t channel quark and therefore a typical range of the interaction is $\sqrt{2}\, M_f^{-1} \approx 0.2$ fm. Changing k_1^2 makes the effective range of the interaction only smaller. Since the derivative of the f wave function is constant over this range, we expect no additional form factors. Of course, this expectation is only valid if the quarks are heavy, corresponding to the basic assumption of the NRQM.

When we go off-mass shell with one of the photons, we observe the onset not only of A_{++}, so that (3.2) will no longer be true, but also that of the A_{+0} amplitude. This amplitude is now no longer forbidden and it will enter with two weight factors: one from the $f_{\gamma\gamma}$ coupling, which we want to illuminate in the following and one from the probability of finding a scalar photon. Let us now turn to the model. The $\gamma\gamma$ - f matrix element (Fig. 2) can be written as

$$V_{f\gamma\gamma} = Tr \int \frac{d^4q}{(2\pi)^4} \; \Psi_f(P,q) \; N(k_i, \varepsilon_i, q, m) \tag{3.3}$$

where q is the relative bound state momentum and $P = k_1 + k_2$. The Bethe-Salpeter amplitude ψ in its rest frame $P = (2m, \vec{0})$ is in the zero binding limit

$$\begin{aligned} \Psi_f(2m,q) &= \frac{2\pi}{i}\,\delta(q_0)\sqrt{2M_f}\; u\left(\frac{P}{2}+q\right)\bar{v}\left(\frac{P}{2}-q\right)\phi_f(\vec{q}) \\ &= -i\sqrt{2M_f}\,(2m)^{-2}\left(\frac{\not P}{2}+\not q+m\right)\not\varepsilon_f\left(\frac{-\not P}{2}+\not q+m\right) \end{aligned} \tag{3.4}$$

and

$$\not{\varepsilon}_f = \frac{\not{P}+M}{2M}\sqrt{\frac{3}{2}}\,\epsilon^{\mu\nu}\hat{q}_\mu\gamma_\nu\,\frac{-\not{P}+M}{2M}\,2\pi\,\delta(q_0)\,\frac{R_f(\vec{q}^{\,2})}{\sqrt{4\pi}} \tag{3.5}$$

We further have

$$N(k_i,\varepsilon_i,q,m) = (-i\not{\varepsilon}_2 e_q)\,\frac{i}{\not{P}/2+\not{q}-\not{k}_1-m}\,(-i\not{\varepsilon}_1 e_q) + \\ + (-i\not{\varepsilon}_1 e)\,\frac{i}{\not{P}/2+\not{q}-\not{k}_2-m}\,(-i\not{\varepsilon}_2 e) \tag{3.6}$$

which we expand to first order in q and insert into (3.3). This now reads ($\not{\varepsilon}_f$ not yet specified and $k \equiv k_2 - k_1$)

$$V_{f\gamma\gamma} = e_q^2\sqrt{3}\sqrt{2M_f}\int\frac{d^3q}{(2\pi)^3}\,\frac{R_f(\vec{q}^{\,2})}{\sqrt{4\pi}}\,M_f^{-2}\,\frac{-1}{k_1\cdot k_2+(m^2-P^2/4)}\,\times$$

$$\times\Big[-P^2(\varepsilon_f\cdot\varepsilon_1\,q\cdot\varepsilon_2+\varepsilon_f\cdot\varepsilon_2 q\cdot\varepsilon_1) \\ +\frac{P^2 k\cdot q}{2k_1\cdot k_2}(\varepsilon_1\cdot\varepsilon_2\,\varepsilon_f\cdot k+2\varepsilon_f\cdot\varepsilon_1 k_1\cdot\varepsilon_2-2\varepsilon_f\cdot\varepsilon_2 k_2\cdot\varepsilon_1) \\ +k\cdot q\,(\varepsilon_f\cdot\varepsilon_2 P\cdot\varepsilon_1-\varepsilon_f\cdot\varepsilon_1 P\cdot\varepsilon_2) \\ +\varepsilon_f\cdot k\,(q\cdot\varepsilon_1 P\cdot\varepsilon_2-q\cdot\varepsilon_2 P\cdot\varepsilon_1) \\ +P\cdot k\,(q\cdot\varepsilon_2\,\varepsilon_f\cdot\varepsilon_1-q\cdot\varepsilon_1\,\varepsilon_f\cdot\varepsilon_2)\Big]\,. \tag{3.7}$$

This is the most general expression to first order in the relative quark momentum q, where we have only used $\varepsilon_f \cdot P = q \cdot P = 0$ (true for on-shell quarks). Strictly speaking it is only valid for a zero width f meson, $P^2 = 4m^2$, since we worked in the zero binding limit. In order to be able to extend the $f_{\gamma\gamma}$ coupling to a physical finite width f meson, we have kept the quark mass wherever this is possible, i.e., in the quark propagator connecting the two photon lines

(compare Fig. 2). In the Bethe-Salpeter amplitude we have to identify m^2 with $P^2/4$. We further assume that the wave function is independent of P^2. This means that we make the smoothest possible continuation of the Bethe-Salpeter amplitude from its on-shell form. We now insert $\not{\epsilon}_f$ and integrate over $\bar{q}$ obtaining

$$V_{f\gamma\gamma} = (320\,\pi\,\Gamma_{f\gamma\gamma}\,M_f^{-3})^{1/2}\,M_f^{4}\;\epsilon^{\mu\nu}\varepsilon_1^{\rho}\varepsilon_2^{\sigma}\;\times$$

$$\times\;\frac{4\,k_1\cdot k_2\,g^{\mu\rho}g^{\nu\sigma} - k^{\mu}k^{\nu}g^{\rho\sigma} - 2k^{\nu}k_1^{\sigma}g^{\mu\rho} + 2k^{\nu}k_2^{\rho}g^{\mu\sigma}}{16\,k_1\cdot k_2\,(k_1\cdot k_2 + m^2 - P^2/4)}\,. \tag{3.8}$$

In terms of the (radial) Schrödinger wave function $R(\bar{q}^2)$

$$\Gamma_{f\gamma\gamma} = \frac{160}{9}\,\alpha^2\,\frac{|R'(0)|^2}{M_f^4}\,. \tag{3.9}$$

The second part of the amplitude is standard

$$V_{f\pi^+\pi^-} = (120\,\pi\,\Gamma_{f\pi^+\pi^-}\,M_f^{-3})^{1/2}\;\epsilon^{\mu\nu}\,q_\mu\,q_\nu \tag{3.10}$$

where q now denotes the difference of the pion momenta.

For ϵ production we find analogously with

$$\not{\varepsilon}_\epsilon = \frac{\not{P}+M}{M}\,\frac{1}{\sqrt{2}}\,(\not{\hat{q}} - \hat{P}\cdot\hat{q}\,\not{\hat{P}})\,\frac{-\not{P}+M}{M}\,2\pi\,\delta(q_0)\,\frac{R_\epsilon(\vec{q}^{\,2})}{\sqrt{4\pi}} \tag{3.11}$$

$$V_{\epsilon\gamma\gamma} = \left(\frac{320}{3}\,\pi\,\Gamma_{\epsilon\gamma\gamma}\,M_\epsilon^{-3}\right)^{1/2}\,M_\epsilon^{4}\;\varepsilon_1^{\rho}\,\varepsilon_2^{\sigma}\,\frac{1}{P^2}\;\times \tag{3.12}$$

$$\times\,\frac{-g^{\rho\sigma}(k^2P^2 - 4k_1\cdot k_2\,P^2 - P\cdot k^2) + 4(k_2^{\rho}k_1^{\sigma}P^2 + (k_2^{\rho}k_1^{\sigma} + k_1^{\rho}k_2^{\sigma})k_1\cdot k_2 - k_2^{\rho}k_2^{\sigma}k_1^2 - k_1^{\rho}k_1^{\sigma}k_2^2)}{16\;\;k_1\cdot k_2\,(k_1\cdot k_2 + m^2 - P^2/4)}$$

instead of (3.8) and

$$V_{\varepsilon\pi^+\pi^-} = (16\pi\,\Gamma_{\varepsilon\pi^+\pi^-} M_\varepsilon^{-3})^{1/2}\; q^2 \tag{3.13}$$

instead of (3.10).

4. THE HELICITY STRUCTURE OF THE $\gamma\gamma f$ VERTEX

In this section we will discuss the helicity structure of the $f - \gamma\gamma$ decay for off-shell photons. We do this for time-like photons to simplify the discussion, and thereby we can study the dipole limit, where $k_1^2 \to M_f^2$, $k_2^2 = 0$. The results can be compared with those of space-like photons and we will discuss this in the context of the full amplitude in Section 6. We only need to do this for the f meson, since the helicity and spin structure of the $\gamma\gamma - \varepsilon$ coupling is trivial.

In Section 3 we have mentioned that only the helicity two amplitude A_{+-} is non-vanishing for the $\gamma\gamma - f$ coupling. This can easily be seen by writing the spin structure of (3.8) in the CM frame of the f meson

$$\begin{aligned} A_{\lambda_1\lambda_2} \sim \epsilon_{\mu\nu}(j_3)\big[& k_1\cdot k_2\, \varepsilon_1^{\mu}(\lambda_1)\, \varepsilon_2^{*\nu}(\lambda_2) + \\ & - k_1^{\mu} k_1^{\nu}\, \varepsilon_1(\lambda_1)\cdot\varepsilon_2^{*}(\lambda_2) + \varepsilon_1^{\mu}(\lambda_1)\, k_1^{\nu}\, \varepsilon_2^{*}(\lambda_2)\cdot k_1 + \\ & - \varepsilon_2^{*\mu}(\lambda_2)\, k_1^{\nu}\, \varepsilon_1(\lambda_1)\cdot k_2\big] \end{aligned} \tag{4.1}$$

and evaluating it with the familiar photon polarization vectors

$$\varepsilon_i(\pm) = \frac{1}{\sqrt{2}}\,(0, \mp 1, -i, 0)$$

and $$\varepsilon_i(0) = \frac{1}{\sqrt{k_i^2}}(k_{i3}, 0, 0, k_{i0})$$

with the polarization tensor of the f meson

$$\varepsilon_0 = \frac{1}{\sqrt{6}} \begin{vmatrix} 0 & & \\ & -1 & \\ & & 2 \end{vmatrix} , \quad \varepsilon_{\pm 1} = \frac{1}{2} \begin{vmatrix} & & 0 \\ & & \mp 1 \\ & & -i \\ 0 & \mp 1 & -i \quad 0 \end{vmatrix} , \quad \varepsilon_{\pm 2} = \frac{1}{2} \begin{vmatrix} 0 & & \\ & 1 & \pm i \\ & \pm i & 1 \\ & & & 0 \end{vmatrix} \tag{4.2}$$

It is sufficient to look at A_{+-}, A_{+0} and A_{++}. One readily finds for $k_1^2 = 0$

$$\begin{aligned} A_{+-} &\sim |\vec{k}_2| \, M_f \\ A_{+0} &\sim \frac{1}{\sqrt{2}} |\vec{k}_2| \sqrt{k_2^2} \\ A_{++} &\sim \frac{1}{\sqrt{6}} |\vec{k}_2| \, k_2^2 \, M_f^{-1} \end{aligned} \tag{4.3}$$

which gives the correct dipole limit as $k_2^2 = M_f^2$. Equation (4.3) is also valid for $k_2^2 > M_f^2$ corresponding to the process $\gamma^* \to f\gamma$. One clearly sees that A_{+0} already becomes especially important at moderate virtual masses of photon 2, because Yang's theorem no longer holds. The "helicity 0" amplitude, however, is much less important at low values of k_2^2.

5. THE ACTUAL CALCULATION

The amplitude of the complete process $e^+e^- \to e^+e^- f \to e^+e^-\pi^+\pi^-$ can now be written down rather easily. Defining

$$T_{\mu\nu}^f = V_{\mu\nu\rho\sigma}^{\gamma\gamma f} \; P_{\rho\sigma\rho'\sigma'}^{\text{spin 2}} \; V_{\rho'\sigma'}^{f\pi\pi} \tag{5.1}$$

with the $V^{\gamma\gamma f}$ vertex taken from (3.8) and the $V^{f\pi\pi}$ vertex from (3.10) the amplitude is given by:

$$A = -e \, \bar{u}(p_3) \frac{\gamma_\mu}{(p_1 - p_3)^2} u(p_1) \, T_{\mu\nu}^f \, \bar{v}(p_2) \frac{\gamma_\nu}{(p_2 - p_5)^2} v(p_5) \tag{5.2}$$

To evaluate the matrix element from this would be straightforward if it were not for the gauge cancellations, which cause the resulting formulae to be numerically unstable. Using the gauge invariance of $T_{\mu\nu}^f$ we can, however, rewrite the electron part:

$$\sum_{\text{Spins}} \bar{u}(p_3)\gamma_\mu u(p_1)\bar{u}(p_1)\gamma_{\mu'} u(p_3) = 8 p_{1\mu} p_{1\mu'} + 2(p_1 - p_3)^2 g_{\mu\mu'} \qquad (5.3)$$

and a similar expression for the positron part.

This reduces the matrix element to

$$\frac{1}{e^4}|A|^2 = \frac{64}{t_1^2 t_2^2}(p_{1\mu} T_{\mu\nu} p_{2\nu})^2 + \frac{16}{t_1^2 t_2} p_{1\mu} T_{\mu\nu} T^{\dagger}_{\nu\mu'} p_{1\mu'} + \frac{16}{t_1 t_2^2} p_{2\nu} T_{\mu\nu} T^{\dagger}_{\nu'\mu} p_{2\nu'} - \frac{4}{t_1 t_2} T_{\mu\nu} T^{\dagger}_{\nu\mu} \quad . \qquad (5.4)$$

The strongest gauge cancellations are present in the first term and can be isolated by introducing the variable $\Delta' = 2\, p_1 \cdot p_2\, P^2 - 4\, p_1 \cdot P\, p_2 \cdot P$ which is related to the variable Δ in Ref. 7). By including this Δ among the phase space integration variables we have removed almost all numerical problems that are related to the gauge cancellations. We would also like to remark here that it is only the structure of the final term of (5.4) that contributes in the case of a Weizsäcker-Williams approximation with unpolarized (massless) photons.

As we wish to study the final $e^+e^-\pi^+\pi^-$ state in various kinematical configurations it is most practical to perform the phase space integrals numerically. A program for the kinematics of the 2γ reaction $e^+e^- \to e^+e^-$ + 2 particles exists[7] and was used here. The only difference between the $e^+e^- \to e^+e^-\mu^+\mu^-$ reaction for which this program was designed and the reaction we are studying here is in the matrix element over which we have to integrate.

To do the same calculation for an ϵ resonance the only change we have to make is to replace $T^f_{\mu\nu}$ by $T^\epsilon_{\mu\nu}$ where $T^\epsilon_{\mu\nu}$ is defined in analogy to Eq. (5.1).

6. RESULTS

To get an impression of what the f signal looks like we calculated various distributions and cross-sections at a beam energy of 15 GeV. As 2γ reactions are usually not very sensitive to the beam energy the results are representative for the energy region in which PETRA and PEP operate. At 15 GeV the total cross-section for the reaction $e^+e^- \to e^+e^- f \to e^+e^-\pi^+\pi^-$ is 357 pb/keV in which the keV refers to the $\gamma\gamma$ width of the f. Results from PLUTO[3] and TASSO[4] put this width in the range of 2-4 GeV, leading to total production cross-sections of about

1 nb. We will, however, quote all cross-sections for a 1 keV width, as this width is an over-all constant and our Monte Carlo calculations are far more accurate than any width measurement that can currently be done for the f.

The full cross-section is of course not readily observable so we studied also the effect of some of the severest cuts on the final state. The severest cut one makes in 2γ physics is when one wishes to see the electron and/or the positron in the final state. The observed cross-section can be very sharply reduced depending on the minimal tagging angle. To illustrate this we calculated the single tag cross-section in which we required the e^+ to be visible and the e^- not to be visible, or $\theta_{e^+} > \theta_{tag}^{min}$ and $\theta_{e^-} < \theta_{tag}^{min}$ for a fixed value of θ_{tag}^{min}. The results are given in Table 1. Such a cross-section drops of course to zero in the limit that θ_{tag}^{min} goes to zero, so for very small tagging angles it is better to know also the inclusive single tag cross-section, i.e., $\theta_{e^+} > \theta_{tag}^{min}$ but no requirements on the e^-. Some of these cross-sections are also given in Table 1. We see that if $\theta_{tag}^{min} = 1^o$ the difference between the two tagging modes is about 10% while at 0.1^o it is about 50%. For larger angles the difference becomes much smaller as it becomes much harder to observe both the e^+ and the e^-.

The next set of cuts that can affect the signal is determined by the observability of the pions. To get a reasonable impression of the effects of angle cuts on the 2π signal we took for each Monte Carlo event the smallest of the four angles $\theta_{\pi^+e^+}$, $\theta_{\pi^+e^-}$, $\theta_{\pi^-e^+}$ and $\theta_{\pi^-e^-}$ where the e^+ and e^- directions indicate here the directions of the incoming e^+ and e^- beams. When experimental acceptance is determined by a finite angle acceptance, it is this variable in which one makes the cut, so it is possible to say from a differential cross-section in this angle θ_π^{min} what fraction of pion pairs will be inside the angular acceptance. Figure 3 shows this fraction as a function of θ_π^{min} both for untagged events and single tagged events with a minimum tagging angle of 5^o. The fact that the curve for the tagged events is lower by a factor of roughly 1.6 over most of the θ_{cut} range is mainly due to the $p_\perp$ of the f when an electron (or positron) is tagged. A smaller part of the effect is due to a modified helicity content of the f when Q^2 becomes large. In our calculation it happens to be rather easy to determine this helicity content as a function of θ_{tag}^{min}. One can make a differential cross-section in terms of the $\cos\theta_\pi^*$ in the $\pi\pi$ (or $\gamma\gamma$) CM frame, where θ_π^* denotes the angle between the outgoing pion and the incoming γ directions. In this distribution the helicity 2 part is proportional to $\sin^4\theta_\pi^*$, the helicity 1 part to $\sin^2\theta_\pi^*\cos^2\theta_\pi^*$ and the helicity 0 part to $(1 - 3\cos^2\theta_\pi^*)^2$. As the f is purely spin 2, the decomposition into these three components is unique. The results are shown in Fig. 4. We would like

to draw the reader's attention to the fact that working with a minimum angle cut means that the results in this graph are basically an average over events in which the electron or positron has a range of θ values, so the point at $\theta_{tag}^{min} = 0$ represents not only events at $Q^2 = 0$ but also events with a larger Q^2. This explains why the helicity 1 and helicity 0 components do not vanish for small θ_{tag}^{min} as suggested by Eq. (4.3). In general many features which one might expect at a fixed tagging angle are shifted to the left in this graph, due to this definition of the tagging angle. In both the limits $Q^2 \to 0$ and $Q^2 \to \infty$ the helicity 1 component has to vanish[13]. This $Q^2 \to \infty$ limit means that the helicity 1 curve should have a maximum which is indeed found in the graph. The $\lambda = 0$ component decreases for increasingly large values of Q^2 because our runs are at finite values of s for the e^+ and e^- beams. This forces the second photon also off-shell once one of the photons develops a really large Q^2. As a consequence one should be very careful to apply arguments that hold for $\gamma^*\gamma$ scattering.

As explained before, part of an f pole could actually be due to the presence of a scalar ε at roughly the same mass. To study such an ε we made Monte Carlo runs similar to those for the f. The mass of this ε was taken[8] to be 1.3 GeV/c^2, its full width 300 MeV/c^2 and the partial width into $\pi^+\pi^-$ was estimated to be 160 MeV/c^2. Even if the ε exists, the uncertainty in these numbers is rather large, and for instance the width could conceivably be smaller. This would not, however, affect the total cross-section too much, only the fraction of the cross-section close to the centre of the peak.

With these parameters as input we obtain a total cross-section for $e^+e^- \to$ $\to e^+e^-\varepsilon \to e^+e^-\pi^+\pi^-$ at 15 GeV beam energy of 251 pb/keV of which 1.40 pb/keV has a single exclusive e^+tag at at least 5°.

To either verify or rule out the presence of such an ε particle one needs to study distributions. From the theoretical point of view the distinction between an f and a mixed f and ε signal is rather simple: one only needs the $\cos\theta$ distribution in the $\pi^+\pi^-$ CM frame. The distributions for both the f and the ε are known -- in the untagged mode the f is almost purely $\lambda = 2$ so this gives a distribution close to $\sin^4\theta_{CM}$ and the ε has a flat distribution -- so the relative ratios can be obtained in a one parameter fit. Unfortunately the experimental situation is not as simple due to a limited pion acceptance. Those pions that are observed are at large θ_{CM} which means that the data are in that region of phase space where it is hard to distinguish $\sin^4\theta_{CM}$ from a constant.

Another way to see an effect could be based on the differences in the pion acceptances due to the different θ_{CM} distributions. This has the advantage of not having to convert an experimental acceptance function to a CM frame.

For this we calculated the equivalent of Fig. 4 for the ε. These curves are presented in Fig. 5. Close study of the differences reveals that angle cuts on the pions are more severe for the ε than for the f. At 45° the difference is about a factor 1.6. One could now compare for instance the number of events within a 45° acceptance with the number of events within a $67\frac{1}{2}^{0}$ acceptance. For the f this ratio is 3.46 while for the ε it is 4.15. The error on these numbers is less than 0.05. For an equal f - ε mixture (after cuts) this would mean a 10% effect. As there is, however, also an electromagnetic background that has to be subtracted one needs rather good statistics for obtaining meaningful results.

It is of course conceivable that with respect to 2 gamma reactions the S*(980) is the dominant NRQM scalar resonance instead of the ε(1300). To detect this would be rather easy as it would give rise to a separate peak. Using M_{S^*} = 980 MeV/c^2, Γ_{tot} = 300 MeV/c^2 and $\Gamma_{S^*\to\pi^+\pi^-}$ = 160 MeV/c^2 we obtain a total cross-section of 640 pb/keV with differential distributions which are very similar to those of the ε(1300). The experimental results do not show this thus far. Their cuts are, however, such that this peak would be sitting on a very fast rising background and could easily be missed.

7. CONCLUSIONS

Calculations of the reaction $e^+e^- \to e^+e^-f \to e^+e^-\pi^+\pi^-$ using the NRQM give results for the production cross-section and differential distributions which are not inconsistent with the early data[3),4)]. If the observed resonance is purely f one obtains a 2γ width for the f of 2 - 4 keV. The theoretical analysis shows a dominance of helicity 2 and a non-negligible fraction of helicity 1 for finite Q^2 of one of the photons, but unfortunately the limited angular acceptance of present experiments makes this component very hard to detect.

Whether an ε resonance is present under the f peak is not easy to tell. Distributions of variables in the laboratory frame may need more statistics than will be available, while the distribution in θ_{CM} suffers from the fact that the experimental acceptance is very small in the region where the difference between the f and the ε becomes obvious. An important step forward would be a positive pion identification to have at least a signal free of backgrounds. Whether this can be done in the near future we do not know.

If the main contribution of the NRQM scalar resonance is in the S^* region it should be easily found experimentally once the experiments are sensitive in this mass region.

Table

$e^+e^- \to e^+e^- f \to e^+e^- \pi^+\pi^-$ cross-sections for various tagging angles and modes. Exclusive means e^+ is observed e^- is not. Inclusive refers to the observation of e^+ without asking questions about the e^-. The errors are due to Monte Carlo statistics.

θ_{tag}^{min} in degrees	mode	$\sigma/\Gamma_{f\gamma\gamma}$ in pb/keV
0.1	excl.	81.9 ± 0.2
0.2	excl.	70.8 ± 0.2
0.5	excl.	50.72 ± 0.14
1.0	excl.	32.27 ± 0.10
2.0	excl.	14.77 ± 0.06
5.0	excl.	2.150 ± 0.011
0.1	incl.	122.1 ± 0.3
1.0	incl.	36.24 ± 0.11
10.0	incl.	0.333 ± 0.002
0	incl.	356.9 ± 0.6

REFERENCES

1) S.J. Brodsky, T. De Grand, J. Gunion and J. Weis; Phys. Rev. Letters 41 (1978) 672; Phys. Rev. D19 (1979) 1418.

2) V.M. Budnev et al.; Phys. Rep. 15C (1975) and references therein.

3) PLUTO Collaboration; Report to the International Workshop on $\gamma\gamma$ Interactions, Amiens, April 1980, Springer Verlag; DESY 80/34 (1980).

4) TASSO Collaboration; Report to the International Workshop on $\gamma\gamma$ Interactions, Amiens, April 1980, Springer Verlag.

5) B. Schrempp-Otto, F. Schrempp and T.F. Walsh; Phys. Letters 36 (1971) 463;
G. Köpp, T.F. Walsh and P. Zerwas; Nucl. Phys. B70 (1974) 461;
P. Grassberger and R. Kögerler; Nucl. Phys. B106 (1976) 457;
J. Babcock and J.L. Rosner; Phys. Rev. D14 (1976) 1286.

6) M. Krammer; Phys. Letters 74B (1978) 361.

7) J.A.M. Vermaseren; Report to the International Workshop on $\gamma\gamma$ Interactions, Amiens, April 1980, Springer Verlag.

8) Particle Data Group; Phys. Letters 75B (1978) 1.

9) C.N. Yang; Phys. Rev. 77 (1950) 242.

10) The first and third reference in 5).

11) M. Krammer and H. Krasemann; Phys. Letters 73B (1978) 50.

12) We calculate $|\mathcal{R}'(0)|^2$ with a "standard" potential model which gives the correct Regge slope for low lying mesons and describes $c\bar{c}$ and $b\bar{b}$ systems, see e.g. H. Krasemann and S.Ono; Nucl. Phys. B154 (1979) 283.

13) The second reference in 5).

FIGURE CAPTIONS

Fig. 1 : $\pi\pi$ resonance production in the quark model (via quark-photon coupling) in the two photon process.

Fig. 2 : The quark model vertex of $\gamma\gamma \to f$.

Fig. 3 : Contributions to the f cross-section by the various helicities as a function of the minimum tagging angle. The single tag exclusive mode was taken.

Fig. 4 : Pion angle cut effects on the f signal, showing the fraction of the signal that is left if an angle cut of θ_π^{cut} is applied to both final state pions. The tagged events were in the exclusive mode (e^+ only).

Fig. 5 : Same as Fig. 4 but now for the ε. The solid line is for the untagged events. The dotted line represents the tagged events ($\theta_{tag}^{min} = 5^o$). For reference we also give the distribution for the untagged f events (dashed line) from Fig. 4.

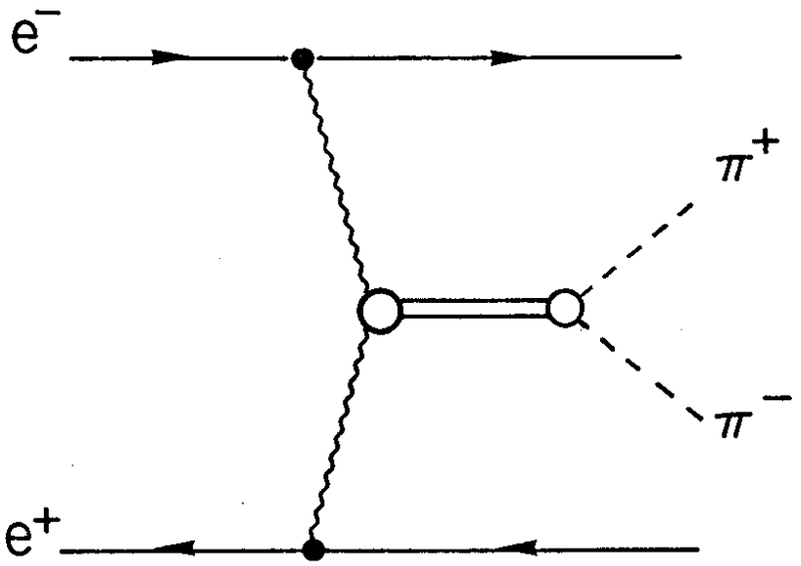

Fig. 1

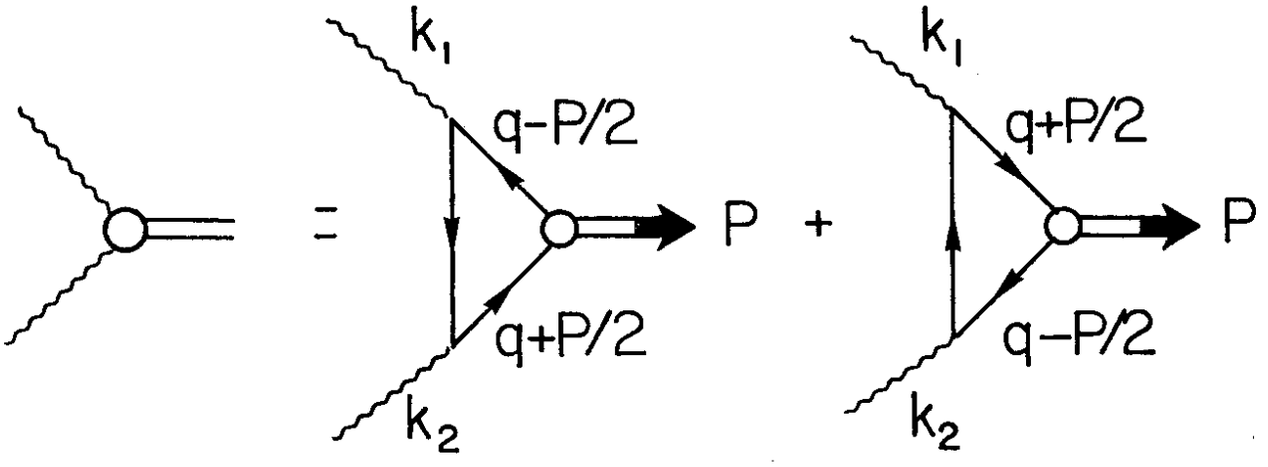

Fig. 2

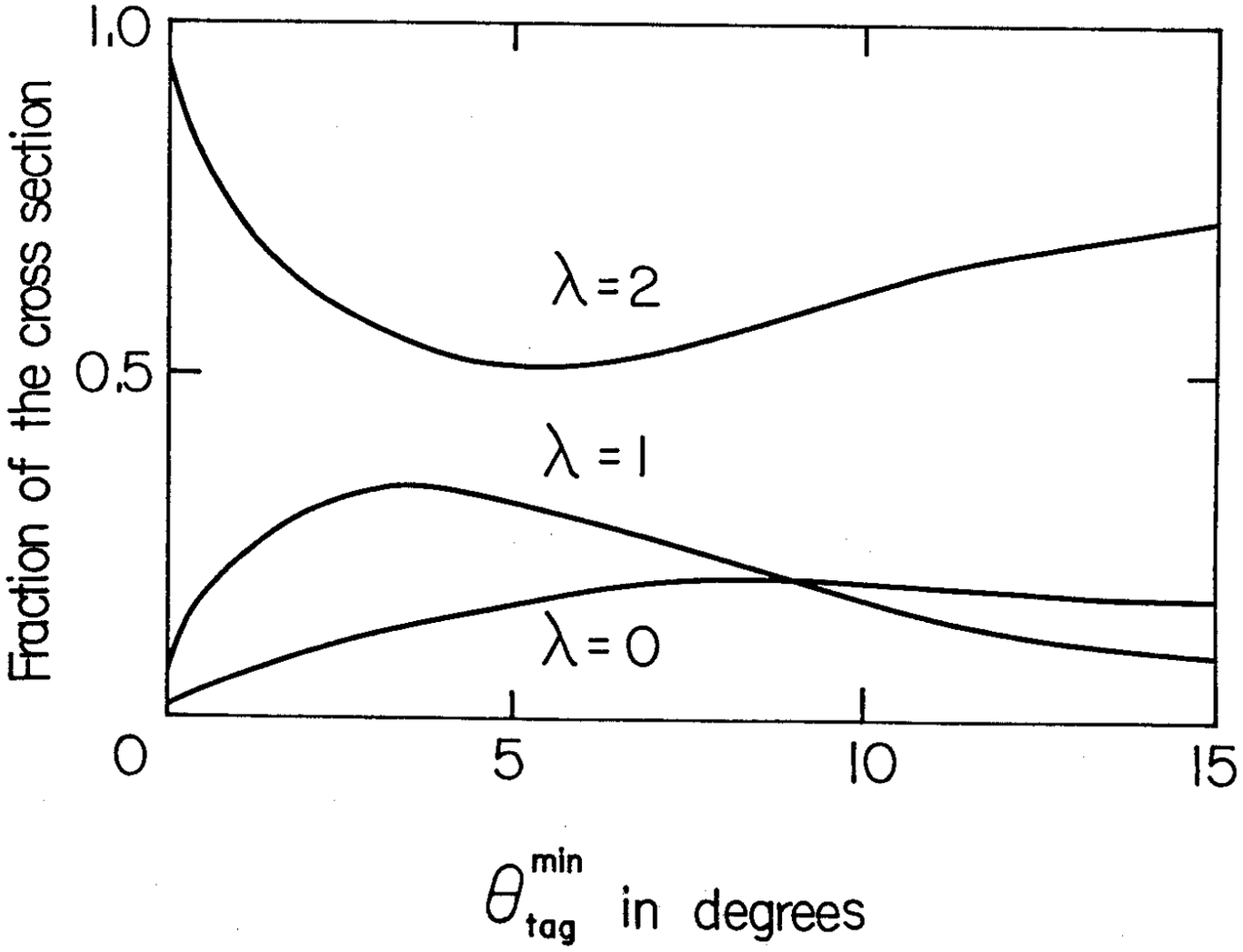
1.0
0.5
0
Fraction of the cross section
λ=2
λ=1
λ=0
0
5
10
15
θ_{tag}^{min} in degrees

Fig. 3

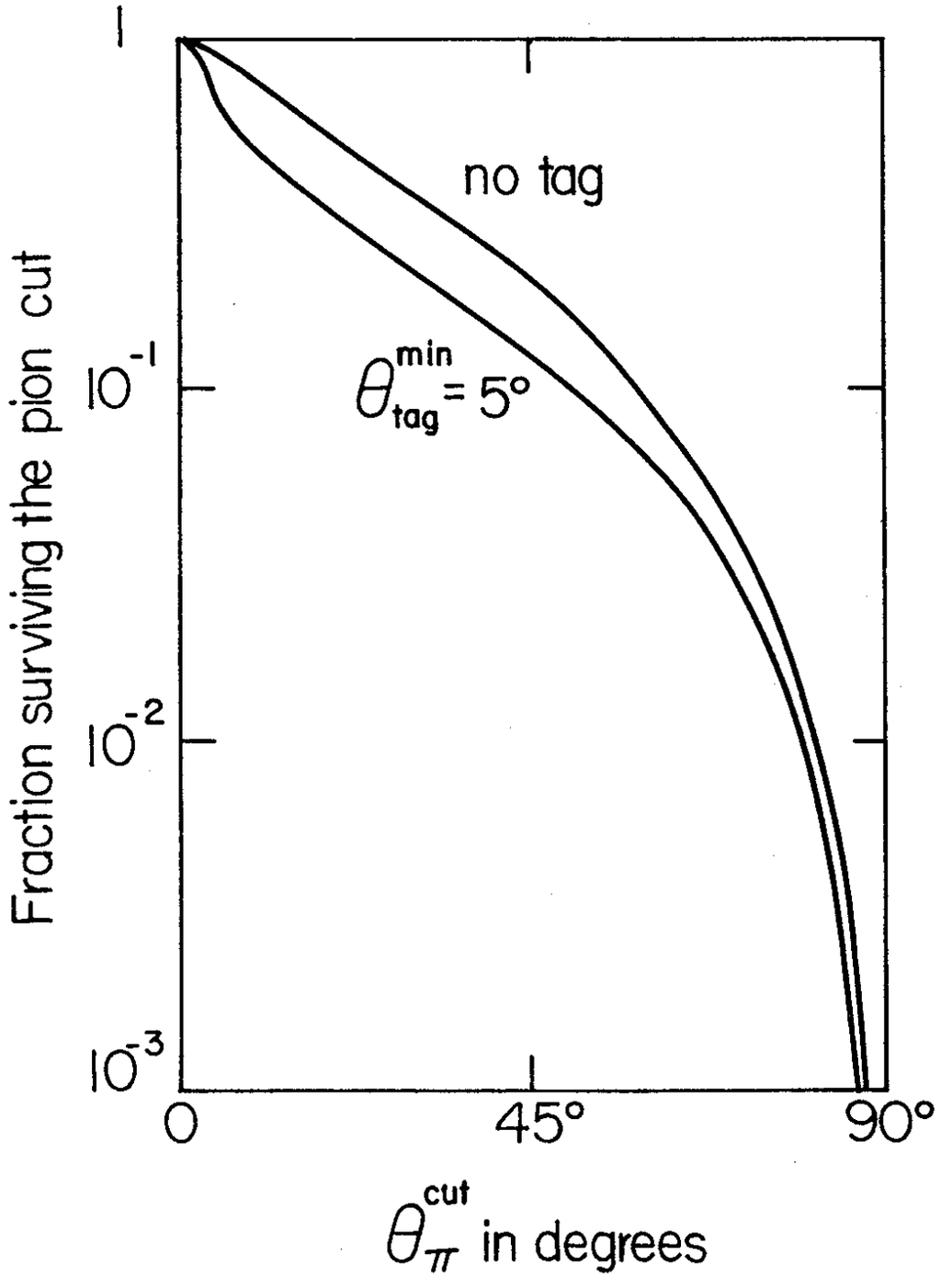
1
10^{-1}
10^{-2}
10^{-3}
Fraction surviving the pion cut
no tag
$\theta_{tag}^{min} = 5°$
0
45°
90°
θ_{π}^{cut} in degrees

Fig. 4

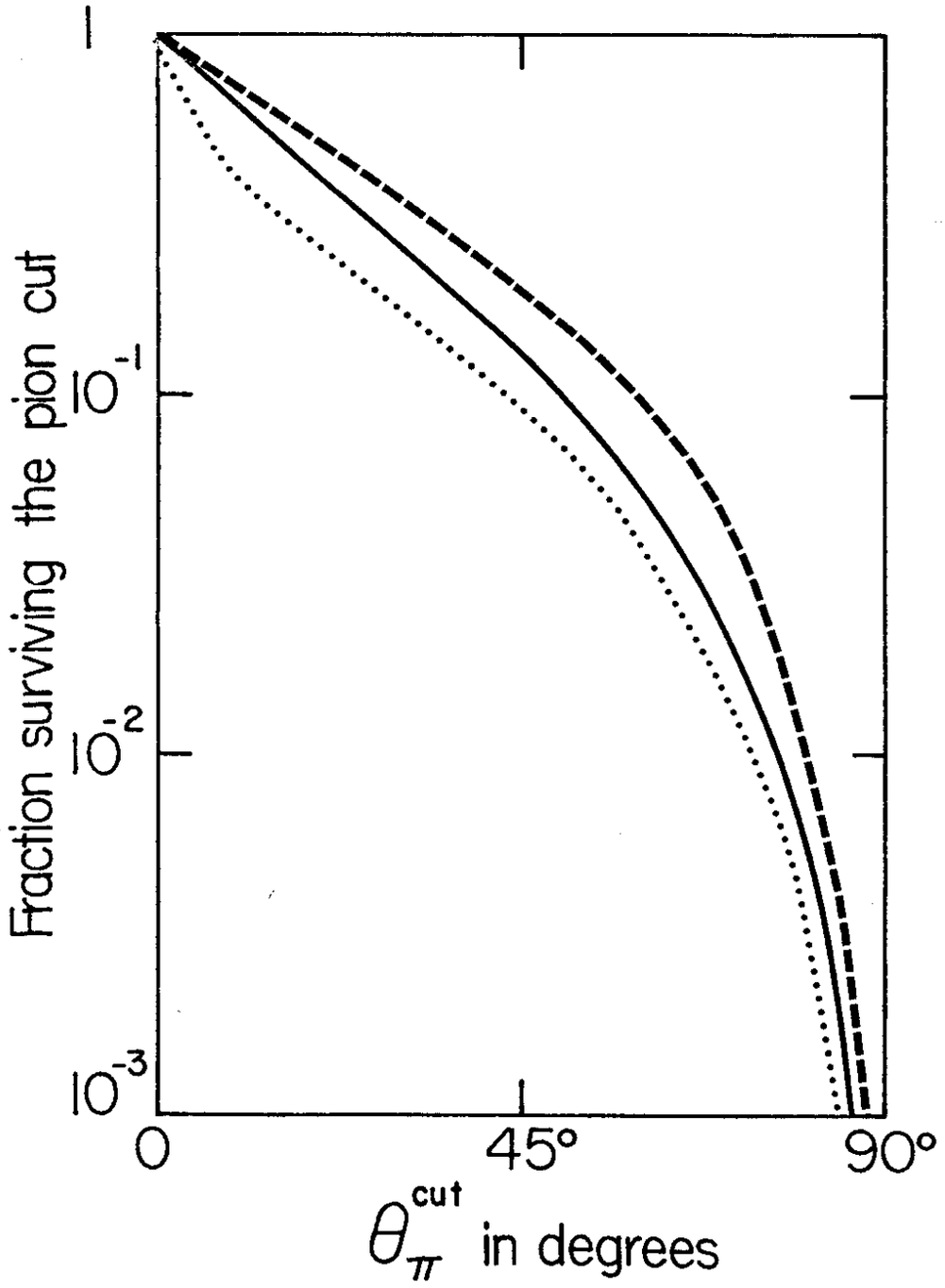
Fraction surviving the pion cut
1
10^{-1}
10^{-2}
10^{-3}
0
45°
90°
θ_{π}^{cut} in degrees

Fig. 5